Supporting Information

Bactericidal Effects of Natural Nanotopography of Dragonfly Wing on *Escherichia coli*

Chaturanga D. Bandara[†,‡], *Sanjleena Singh*[§], *Isaac O. Afara*[ï], *Annalena Wolff*[§], *Tuquabo Tesfamichael*[*§], *Kostya (Ken) Ostrikov*[‡,§], *Adekunle Oloyede*[†ï]

[†]School of Chemistry, Physics and Mechanical Engineering, Science and Engineering Faculty, Queensland University of Technology (QUT), Brisbane, Queensland 4001, Australia

[‡]Institute for Health and Biomedical Innovation (IHBI), Queensland University of Technology (QUT), Kelvin Grove, Queensland 4059, Australia

[§]Institute for Future Environments, Queensland University of Technology (QUT), Brisbane, Queensland 4001, Australia

[ï]Research and Innovation Centre, Elizade University, 1 Wuraola Ade.Ojo Avenue, P.M.B 002, Ilara-Mokin, Ondo State, Nigeria

Email: t.tesfamichael@qut.edu.au

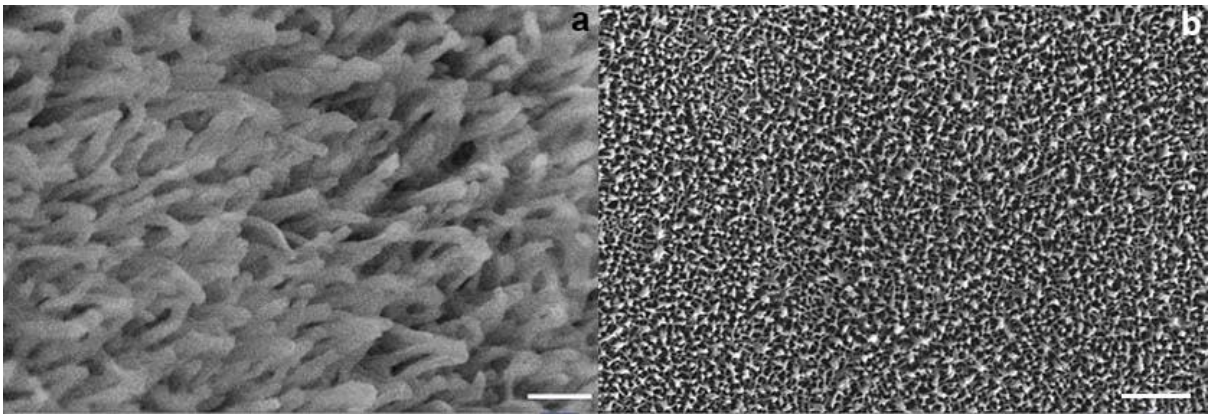

Figure S1: SEM images of dragonfly wing. (a) 1 nm thick Cr coated dragonfly wing showing nanopillars are at single height. Low depth of focus in SEM cause blurring of nanopillars away from plane of focus. Scale bar 200 nm (b) 10 nm gold coated dragonfly wing show nanopillar topography Scale bar 1 μm

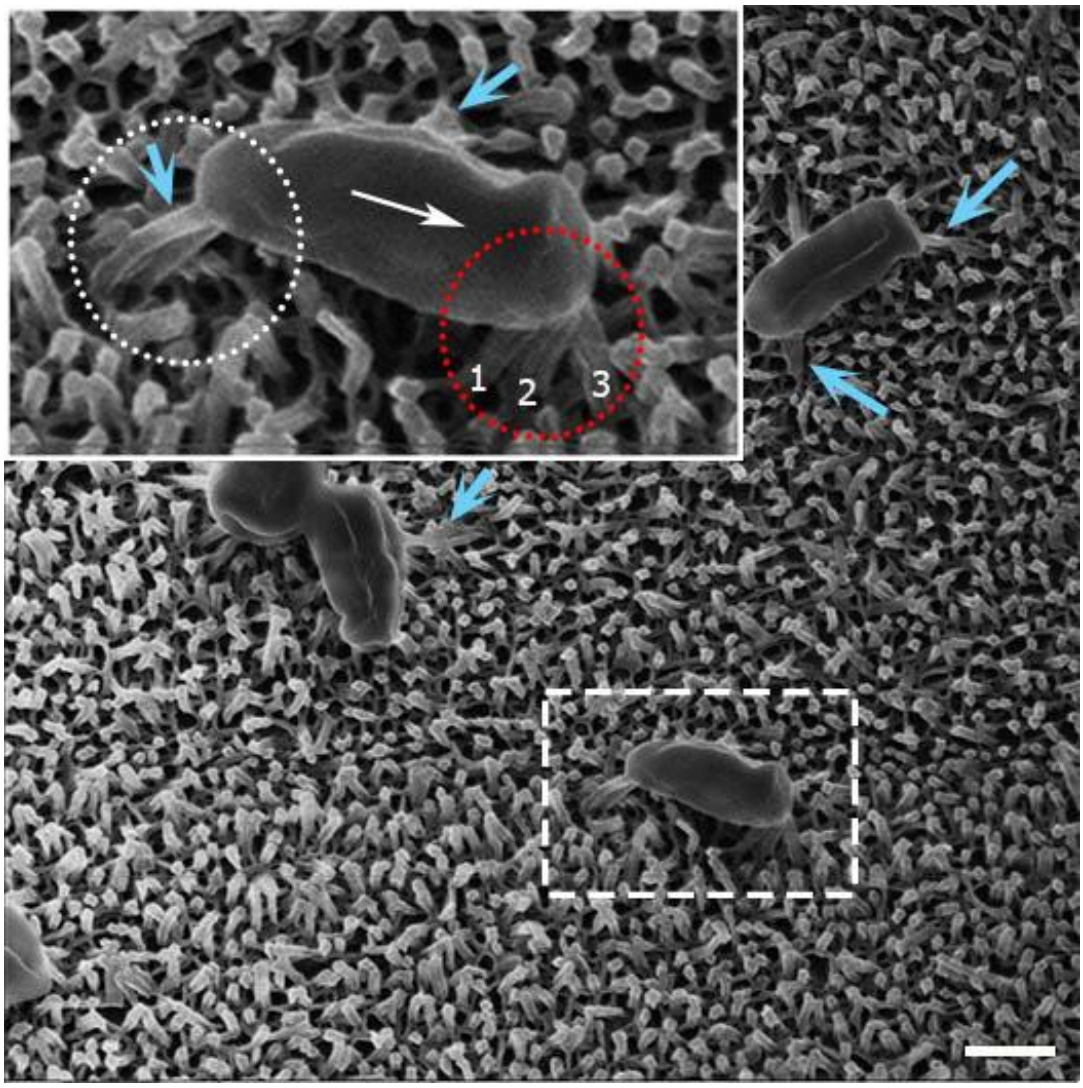

Figure S2: HIM micrograph show *Escherichia coli* bacterium attempts to move on nanopillars of dragonfly wing. Secreted EPS by bacteria during adhesion is pointed by blue arrows. At this larger field of view (FOV), these EPS secretions are not dominantly seen. Adhesion of bacteria to nanopillars has caused bending nanopillars to the direction of movement. Inset shows magnified area. Bent nanopillars in front are circled in red. Front side nanopillars are pushed and back side nanopillars with EPS are stretched (white circle). White arrow shows the direction which bacterium attempt to move. Other bacteria show the secreted EPS to attach on to the nanopillars. Scale bar 500 nm

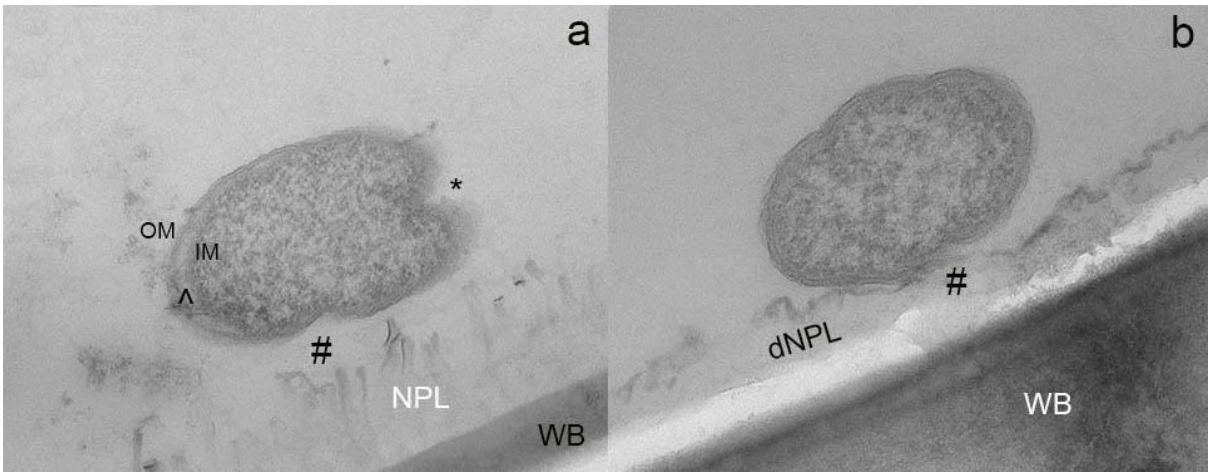

Figure S3: TEM tomograph compare interfaces of bacteria on nanopillar topography and a damaged area (no nanopillars) of dragonfly wing. (a) *E. coli* on nanopillar layer (NPL) and b) *E. coli* on damaged nanopillars (dNPL) of dragonfly wing. When nanopillars are present, a gap between membrane and nanopillars (#) at interface, separation of inner and outer membranes (^) and membrane deformations (∗) are evident. When nanopillars are damaged, a gap (#), membrane deformations or separation of bacterial membranes are not present. This indicates bacterium experience more stress on a nanopillar surface, compared to a surface without nanopillars. Therefore more EPS is secreted on a nanopillar surface (a) compared to a flat surface (b). Therefore gap is greater where nanopillars are present.

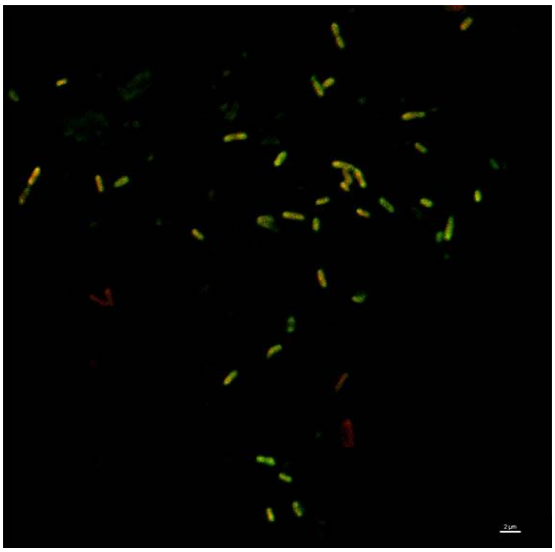

Figure S4: Confocal micrograph of live/dead staining of *Escherichia coli* on dragonfly wing. All cells are stained in red or yellow color. This confirms all cells are dead and their membranes are ruptured. Scale bar 2 μm

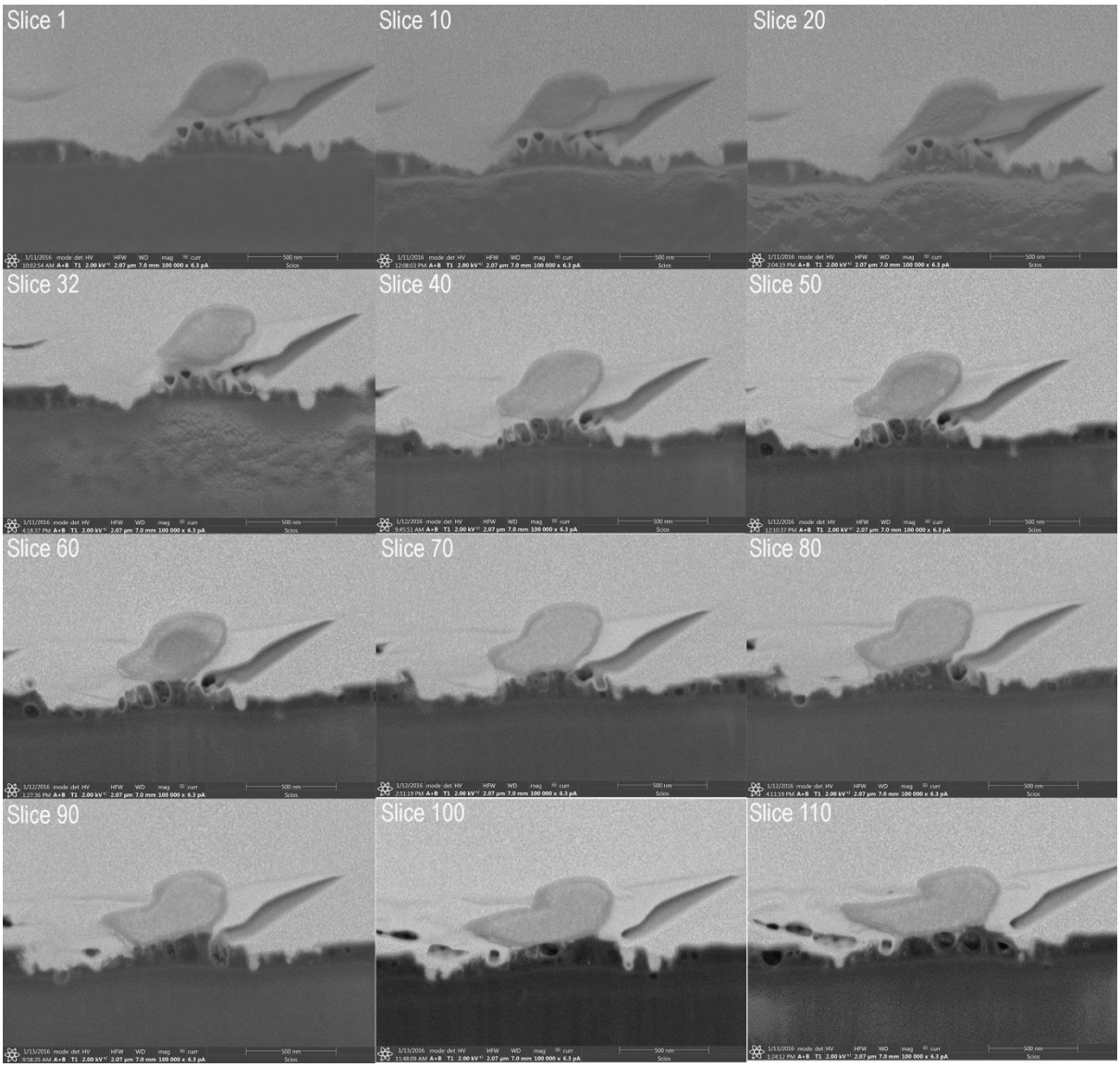

Figure S5: FIB/SEM data showing interface. Data shown at every 10 slice. These data were used to reconstruct 3D interface in Figure 6.

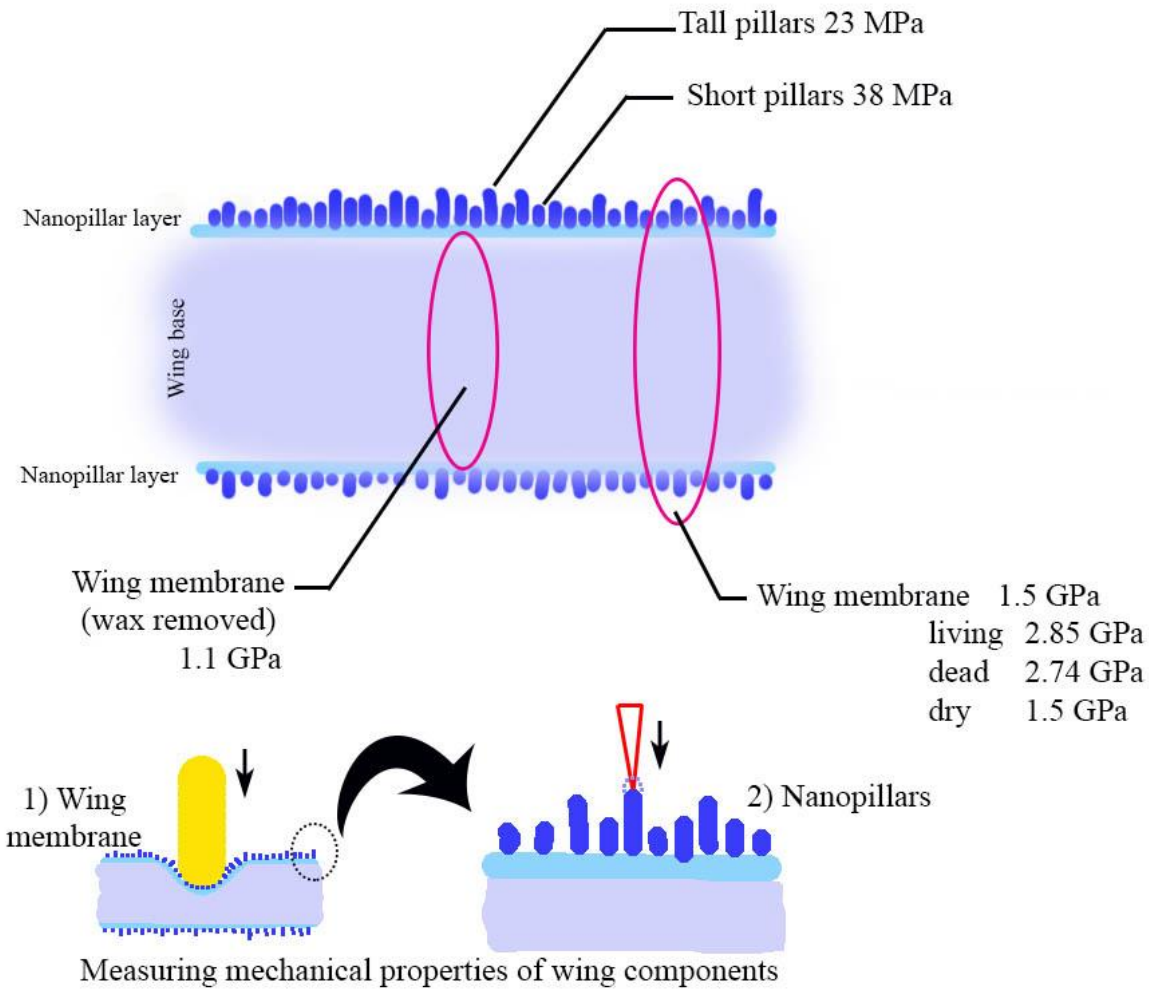

Figure S6: Comparison of mechanical properties reported in different wing components. 1) Previous studies reported the mechanical properties of the wing membrane. This study reports the mechanical properties of the nanopillars on dragonfly wing.

Advantages and limitations of AFM and TEM approach for measuring the height of high aspect ratio surface features.

AFM is one of the most commonly used methods to characterize the surface topography in general. However, when AFM is used to characterize high-aspect ratio topography as found in our sample, it requires a special high-aspect ratio cantilever. In AFM measurements, surface is characterized from top to the bottom. This setup requires the movement of cantilever from the top to the bottom, otherwise it will report the height as the depth which cantilever can travel. In a situation where surface features are densely packed, this characterization is even challenging and could lead to disturb the movement of cantilever tip to the bottom, reporting false measurements in the height measurements. Therefore the optimum measurement requires a sharp tip. This is illustrated in the Figure S7.

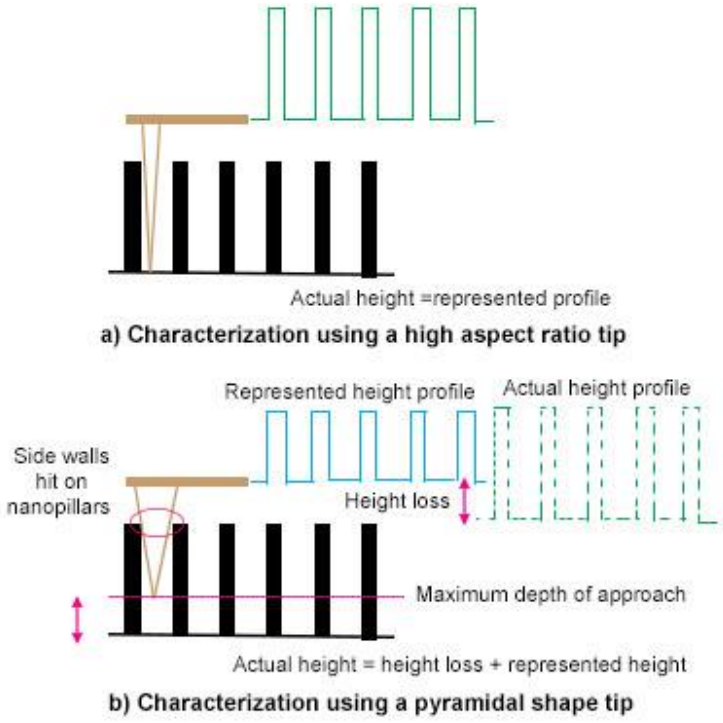

Figure S7: Limitation of AFM characterization when characterizing a high aspect ratio surface with pyramidal tip.

In this experiment, we use AFM to measure and map the mechanical properties of individual nanopillars while characterizing the topography, so the topography and its mechanical properties can be related to each other. Therefore, we have used a cantilever which can measure the mechanical properties while resolving the surface topography. As the triangular shaped cantilever tip used here is not designed for characterizing high-aspect ratio surfaces, the tip may not travel the entire height scale of nanopillars, but stops in midway as the expanding side walls of AFM tip can approach on to adjacent nanopillars while descending through the gap of two nanopillars. With the PeakForce tapping AFM, where Z movement is governed by the adhesion force at tip, this type of interference from adjacent pillars can influence the advancement of cantilever tip to

the bottom of nanopillars. However, this interference does not have an effect on the mechanical property measurement of the nanopillars.

In TEM, it images the cross-section, hence such limitation in AFM is not possible. There is a potential limitation associated in TEM measurements as the samples do not cut through the center of each pillar during sample preparation. As electrons are transmitted through a 100 nm thick lamella, it is not required to cut through the middle of a nanopillar. Secondly, the prepared TEM lamellas were 100 nm thick while the nanopillars are mostly about 40 nm in diameter. For this reason, there is a high chance of the entire nanopillar to be within a TEM cross-section rather than chance of a tiny slice of nanopillar trapped in the TEM lamella during the measurement. Therefore, use of TEM is associated with less errors despite the position of cross-section compared to AFM measurements to determine the height of nanopillars.

Table S1: Natural nanotopographies and their bactericidal efficiencies reported

Reference	Substrate	Shape	Uniformity	Dimensions	Cells tested	Killing efficiency	Main findings
Ivanova et al.[1] (2012)	Cicada wing	pillar	regular	d=100 nm at base, 60 nm at cap h= 200 nm, λ= 170 nm	*Pseudomonas aeruginosa* (ATCC 9027)	not tested	Take 220 s to occur membrane damage Bactericidal activity is physico-mechanical effect.
Hasan et al.[2] (2012)	Cicada wing	pillar	regular		*Bacillus subtilis* *Staphylococcus aureus* *Planococcus maritimus* *Branhamella catarrhalis* *Escherichia coli*	resistant resistant resistant efficiency not given efficiency not given efficiency not given	Kill Gram-negative cells only, Gram-positive cells are resistant

					Pseudomonas fluorescens	6.1±1.5x10^6 cells in 30 min	
					Pseudomonas aeruginosa		
Ivanova et al.[3] (2013)	Dragonfly wing *D. bipunctata*	pilla r	random	d<90 nm, many below 30 nm h=240 nm, λ=200-1800 nm	*Pseudomonas aeruginosa*	3.0 x 10^5	Nanopillars of dragonfly wings are highly bactericidal against Gram-negative, Gram-positive bacteria and endospores
					Staphylococus aureus	4.6 x 10^5	
					Bacillus subtilis spores	1.4 x 10^5	
						~1.0 x 10^5	
Kelleher et al.[4] (2015)	Cicada wing 1	Pilla r		d = 156 nm, h = 241 nm λ=165 nm	*Pseudomonas fluorescens*	0.222	Pitch and diameter of pillars effect bactericidal property
	Cicada wing 2	Pilla r		d = 159 nm, h = 182nm		0.123	
						0.0067	

			λ=187 nm		(Dead:live ratio)	
	Cicada wing	pilla r	d = 207 nm, h = 182 nm λ=251 nm			
	3					
Mainwaring et al.[5] (2016)	Dragonfly wing of *H. papuensis*	pilla r	random d = 80 nm, h = 200-300 nm, λ = 180 nm	*Pseudomonas aeruginosa* *Staphylococus aureus* *Bacillus subtilis*	*H. papuensis* and *H. papuensis* <10x10^4 *D. bipunctata* 13-47x10^4 cells cm^{-2} min^{-1} over 3 h	Changes to topography result in substantial changes in bactericidal activity and their behaviour may also influence the bactericidal efficiency
	Dragonfly wing of *H. papuensis*	pilla r				
	Dragonfly wing of *D. bipunctata*	pilla r				

Table S2: Fabricated nanotopographical surfaces and their bactericidal efficiencies reported

Reference	Substrate	Shape(s)	Regularity	Dimensions	Cells tested	Killing efficiency	Main findings
Ivanova et al.[3] (2013)	SiO_2	pillar	random	d<90 nm, many d=20-80 nm bimodel, h= 500nm, λ=200-1800 nm	*Pseudomonas aeruginosa* *Staphylococcus aureus* *Bacillus subtilis* Spores	4.3 x 10^5 4.5 x 10^5 1.4 x 10^5 ~0.7 x 10^5 cells	Dragonfly wing and black Si surface nanoarchitecture is complex compared to cicada wing. Both surfaces have independent chemical compositions and are highly bactericidal against Gram-negative, Gram-positive bacteria and endospores.

						cm^{-2} min^{-1} over 3 h	
Dickson et al.[6] (2015)	PMMA	pillar	regular		*Escherichia coli*	16-141%	Optimal nanopillar spacing to kill bacteria is 130-380 nm
Yee et al.[7] (2015)	PMMA	Cicada wing replica	regular	d = 60nm, h = 200 nm λ=170 nm	*Escherichia coli*	~22%	Nanostructures were created on PMMA using nanoimprint lithography.
		Flat surface		N/A		~7%	Imprinted polymer nanostructures can prevent bacteria adhesion without chemical modifications to the polymer surface
		pillar		d = 267nm, h =		~12%	

	300 nm λ=692 nm		
pillar		~10%	
	d = 215nm, h =		Dead bacterial cells are longer
	300 nm λ=595 nm		than live cells
pillar		~17%	
	d = 190nm, h =		
	350 nm λ=320 nm		
Square		Not	
pillar	d = 442nm, h =	given	
	300 nm λ=848 nm		
Square			
pillar	d = 139nm, h =	Not	
	300 nm λ=278 nm	given	

Bhadra et al.[8] (2015)	Titanium	nano-wire array	random		*Pseudomonas aeruginosa* *Staphylococcus aureus*	50% 20%	Hydrothermally etched titanium surfaces show bactericidal activity and survival of primary human fibroblasts on surface
SjÖstrÖm et al.[9] (2016)	Ti alloy	spikes	random	d=20 nm, h and λ not given	*Escherichia coli* (K12)	40% reduction of viability	By annealing the Ti alloy surfaces, it is possible to grow vertically aligned nanospikes with bactericidal properties
Fisher et al.[10] (2016)	Diamond	cone	Uniform and random				Random array show enhanced bactericidal ability over uniform and highly dense nanocone surface

References

1. Ivanova, E. P.; Hasan, J.; Webb, H. K.; Truong, V. K.; Watson, G. S.; Watson, J. A.; Baulin, V. A.; Pogodin, S.; Wang, J. Y.; Tobin, M. J.; Löbbe, C.; Crawford, R. J., Natural Bactericidal Surfaces: Mechanical Rupture of Pseudomonas Aeruginosa Cells by Cicada Wings. *Small* **2012,** *8*, 2489-2494.
2. Hasan, J.; Webb, H. K.; Truong, V. K.; Pogodin, S.; Baulin, V. A.; Watson, G. S.; Watson, J. A.; Crawford, R. J.; Ivanova, E. P., Selective Bactericidal Activity of Nanopatterned Superhydrophobic Cicada Psaltoda Claripennis Wing Surfaces. *Appl. Microbiol. Biotechnol.* **2012,** *97*, 1-6.
3. Ivanova, E. P.; Hasan, J.; Webb, H. K.; Gervinskas, G.; Juodkazis, S.; Truong, V. K.; Wu, A. H.; Lamb, R. N.; Baulin, V. A.; Watson, G. S.; Watson, J. A.; Mainwaring, D. E.; Crawford, R. J., Bactericidal Activity of Black Silicon. *Nat Commun* **2013,** *4*, 2838.
4. Kelleher, S. M.; Habimana, O.; Lawler, J.; O' Reilly, B.; Daniels, S.; Casey, E.; Cowley, A., Cicada Wing Surface Topography: An Investigation into the Bactericidal Properties of Nanostructural Features. *ACS Applied Materials & Interfaces* **2015**.
5. Mainwaring, D. E.; Nguyen, S. H.; Webb, H. K.; Jakubov, T.; Tobin, M.; Lamb, R.; Wu, A. H.-F.; Marchant, R.; Crawford, R. J.; Ivanova, E. P., The Nature of Inherent Bactericidal Activity: Insights from the Nanotopology of Three Species of Dragonfly. *Nanoscale* **2016**, *6*, 6527-6534.
6. Dickson, M. N.; Liang, E. I.; Rodriguez, L. A.; Vollereaux, N.; Yee, A. F., Nanopatterned Polymer Surfaces with Bactericidal Properties. *Biointerphases* **2015,** *10*, 021010.
7. Yee, A. F. I., CA, US), Liang, Elena (Irvine, CA, US), Nicole, Ing. (Irvine, CA, US), Gibbs, Markelle (Irvine, CA, US), Dickson, Mary Nora (Irvine, CA, US) Bactericidal Surface Patterns. 2015/10/01, **2015**.
8. Bhadra, C. M.; Khanh Truong, V.; Pham, V. T. H.; Al Kobaisi, M.; Seniutinas, G.; Wang, J. Y.; Juodkazis, S.; Crawford, R. J.; Ivanova, E. P., Antibacterial Titanium Nano-Patterned Arrays Inspired by Dragonfly Wings. *Sci. Rep.* **2015,** *5*, 16817.
9. Sjöström, T.; Nobbs, A. H.; Su, B., Bactericidal nanospike surfaces via thermal oxidation of Ti alloy substrates. *Mater. Lett.* **2016,** *167*, 22-26.
10. Fisher, L. E.; Yang, Y.; Yuen, M.-F.; Zhang, W.; Nobbs, A. H.; Su, B., Bactericidal Activity of Biomimetic Diamond Nanocone Surfaces. *Biointerphases* **2016,** *11*, 011014.